Global NEST Journal, Vol 25, No 9, pp 111-126

Chemically modified Ascophyllum nodosum seaweed: a sustainable solution for heavy metal removal from wastewater

Selvakumar D.[1]*, Thiru S.[2], Ezhilkumar M.R.[3] and Yuvaraja R.
[1]Department of Civil Engineering, Shanmuganathan Engineering College, Pudukottai–622507, Tamil Nadu, India
[2]Department of Mechanical and Materials Engineering, University of Jeddah, Jeddah–21959, Kingdom of Saudi Arabia
[3]Department of Civil Engineering, Sri Krishna College of Engineering and Technology, Coimbatore–641008, Tamil Nadu, India
[4]Department of Civil Engineering, Velammal College of Engineering and Technology, Madurai–625009, Tamilnadu, India
Received: 26/07/2023, Accepted: 02/09/2023, Available online: 19/09/2023
*to whom all correspondence should be addressed: e-mail: selvabakkiya@gmail.com
https://doi.org/10.30955/gnj.005258

Graphical abstract

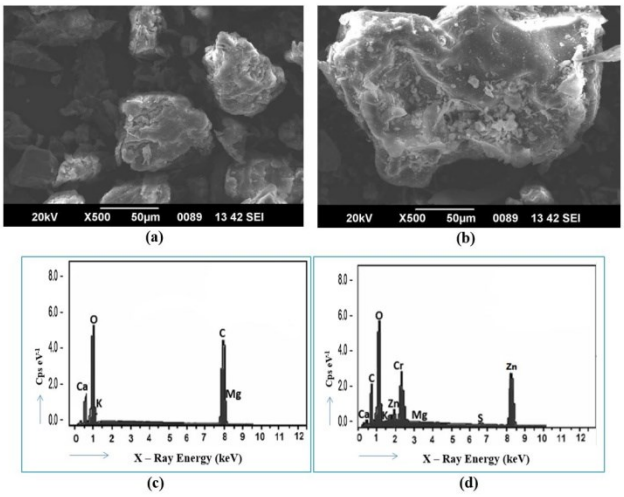

Abstract

In this study, a batch adsorption process was conducted utilizing Ascophyllum nodosum biosorbent as an organic adsorbent used for the elimination of heavy metal ions (specifically chromium, nickel, and zinc) from wastewater. To examine the surface morphology and functional groups, the biosorbent underwent analysis using FTIR, SEM & EDX technologies. To understand the nature of the adsorption process, several isothermal studies were conducted. These studies aimed to determine whether the adsorption process was homogeneous or heterogeneous in nature. Furthermore, the physical or chemical nature of the metal ion adsorption on the adsorbent was investigated through kinetic studies. Thermodynamic investigations were also carried out to assess whether the adsorption of metal ions was exothermic or endothermic, as well as to conclude the spontaneity of the process. Notably, the findings indicated that the inclusion of 0.3N HCl resulted in the highest rate of desorption, indicating its effectiveness in releasing the adsorbed metal ions. The AN – Brown Algae adsorbs targeted metal ions (Cr(VI), Ni(II), Zn(II)) at percentage of 93.55%, 87.56% and 83.27% respectively from the synthetic solution under the optimum conditions in batch study.

Keywords: Biosorption, Ascophyllum nodosum, heavy metals, isotherm & kinetic studies, thermodynamic studies, desorption

1. Introduction

Water pollution is a significant problem that we have been dealing with for a long time. It is essential to have clean water for communities, animals, plants, and industrial processes. The supply of uncontaminated water is a critical challenge, and many countries are conducting extensive research to mitigate these issues using various techniques. Recently, water has become highly polluted due to intense industrial manufacturing and other harmful activities. As a result, its physical and chemical properties change, rendering it unsuitable for drinking. Several factors contribute to the polluting of water. The presence of metal ions, dissolved solids, suspended solids, organic and non-organic pollutants can all make water seem polluted (Yogeshwaran *et al*, 2021). These pollutants can originate from industrial activities, agricultural runoff, domestic wastewater, and other sources. Among these pollutants, heavy metal pollution is a significant concern due to the toxicity and accumulation of metal ions, posing a serious threat to both the environment and human health. The increase in heavy metal pollution has led to a variety of health concerns, such as cancer, respiratory problems, and various illnesses. It is very difficult to eliminate the heavy metal contamination from the wastewater before getting discharged to the water resources (Venkatraman *et al*, 2021). Efficient methods for eliminating heavy metal ions from wastewater have been widely researched and devised. For the elimination of metal ions through batch adsorption, considerable attention has been given to the adsorption process arising from the urgent need for a breakthrough treatment process. This method offers several advantages, including cost-effective method for targeted removal of specific

metals, and the ability to desorb without generating sludge.

Adsorption is a phenomenon in which particles, electrically charged entities, or volatile compounds gather on the surface of an adsorbent material, either in a discontinuous manner or within a stationary column (Yahya *et al*, 2020). To remove toxic metal ions from water through adsorption process using various adsorbent materials, both natural and derived from industrial waste. Often, these adsorbent materials are transformed into activated carbon to enhance the efficiency in capturing adsorbate (Labied *et al*, 2018). The heavy metals and its concentration level was decreased through the adsorption process using various organic/inorganic substances. These natural materials possess adsorption properties that enable them to effectively capture and immobilize metal ions, thereby reducing their concentration in water. By utilizing these natural adsorbents, it is possible to develop sustainable and environmentally friendly methods for treating water contaminated with metal pollutants (Fakhar *et al*, 2021). In this study, the application of Ascophyllum nodosum microalgae, a natural organic material, is being employed to address the issue of heavy metallic ions contamination in aqueous solutions, effectively removing such contaminants.

Ascophyllum nodosum (AN), commonly known as knotted wrack, is characterized by its long, tough, and leathery fronds. The fronds are irregularly dichotomously branched, meaning they divide into two branches in an irregular pattern. Along the fronds, large, egg-shaped air bladders are present, arranged at regular intervals and not stalked (Katiyar *et al*, 2021). These fronds can grow up to 2 meters in length and are anchored to rocks and boulders by a holdfast, which provides stability and attachment. The consumption of Ascophyllum nodosum has been shown to provide dental benefits in humans, dogs, and cats. Additionally, it is consumed by both humans and animals as a nutritional supplement, owing to its various health-promoting properties (Lin *et al*, 2020). Ascophyllum nodosum has been chosen as a suitable option for water treatment, particularly in the removal of heavy metal ions. Extensive research studies have been conducted to investigate the efficacy of different seaweeds in the process of extracting heavy metal ions from water-based solutions. Increasing levels of heavy metal pollution have given rise to various health problems, including cancer, respiratory issues, and other ailments. Therefore, it is of utmost importance to decrease or eliminate the concentration of heavy metal ions prior to its release into natural water sources. Significant efforts have been dedicated to investigating this matter and devising efficient techniques to eliminate heavy metallic ions from wastewater.

2. Materials and methods

2.1. Examine of adsorbent

The Ascophyllum nodosum (AN) adsorbent, also known as Brown Algae seaweed, collected from Ramanathapuram district, India. The double distilled water was used to wash the collected AN seaweed for removing the impurities. Then the AN seaweed was dried using the sunlight for a period of two weeks. Using 1 HP Micro active motor, the dried AN seaweed was crushed for several times and sieved in the range from 125 to 150 µm. The final crushed AN seaweed powder has been taken for further experimental studies. To further eliminate impurities, the crushed AN biochar was subjected to an oven at 140°F for a day.

2.2. Preparation of metal ion solutions

To prepare the stock solutions of potassium dichromate ($K_2Cr_2O_7$), nickel sulphate ($NiSO_4$), and zinc chloride ($ZnCl_2$), each compound was dissolved in 1 liter of double-distilled water at a concentration of 100 mg per liter. This resulted in the formation of concentrated solutions of the respective compounds, which were used for further experimentation and dilution as required. To obtain different desired concentrations, the stock solutions were then diluted with additional double-distilled water.

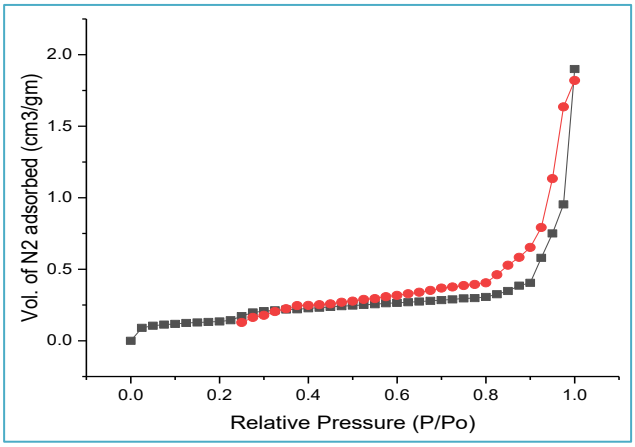

Figure 1. BET surface area analysis by nitrogen adsorption & desorption

Table 1. Pore properties of rice straw adsorbent material

S. No.	Type of property	Calculated value
1.	Surface area	534 m^2/g
2.	Pore volume	0.254 cm^3/g
3.	Pore radius	75.934 Å
4.	Surface area (BET)	27.384 m^2/g
5.	Average pore diameter	nm

2.3. BET surface area and pore distribution

The Ascophyllum nodosum (AN) charcoal was analysed using the adsorption-desorption isotherm technique with nitrogen at -196°C. This analysis was conducted to determine the pore diameter, BET surface area, and volume of micro and meso pores of the biosorbent. The nitrogen adsorption-desorption rate of the biosorbent is shown in Figure 1, and the characteristics of the biosorbent are summarized in Table 1. The isotherms displayed shows the presence of both micro and meso pores and it indicates the type II category of isotherm studies. The initial part of the isotherm plot represents the micro pores, where the adsorption occurs in the form of a monolayer on the surface of the biosorbent (Nadir *et al*, 2020). The latter part of the plot, at higher relative pressure, indicates the adsorption of multilayers in the

meso pores, which are larger pores within the biosorbent structure. The biosorbent exhibited a BET surface area of approximately 534 m^2/g, which is relatively lower compared to the BET surface area of other commercially available activated carbons.

2.4. Batch adsorption studies

A batch mode approach was employed to conduct the adsorption of heavy metal ions onto the adsorbent. The experimental conditions were manipulated by altering the parameters of acidity (pH), duration of contact, quantity of adsorbent used, concentrations of metal ions, and temperature. To assess the extraction of heavy metal ions, a solution of 100 mL was prepared, containing a concentration of 50 mg/L for each respective metallic ion. The treatment process was then applied to this solution. Up to neutral stage, the pH level of the synthetic solution was adjusted, and the temperature was maintained at 30°C throughout the experiment. By varying the pH and monitoring the metal ion removal, the influence of pH on the effectiveness of the treatment process could be assessed. The equilibrium period for each experiment was 60 minutes. The AN biochar dose was gradually added (0.5 to 2.5 g/L) into the metal ion containing solution and the effect of increasing adsorbent dose has been investigated. By increasing the amount of biosorbent and analysing the metal ion removal, the relationship between adsorbent dosage and its efficacy in removing heavy metal ions could be examined. Conical flasks containing the solution and adsorbent were placed on a rotary shaker and agitated for 60 minutes to ensure equilibrium was achieved. The time of interaction between metal ions and the AN biosorbent was increased up to 1 hour with an interval of 10 minutes. During the contact time, the Equation 1 was used to discover the quantity of Cr, Ni and Zn uptake by the AN biosorbent. This allowed for the determination of the adsorption capacity and efficiency of the adsorbent in removing heavy metal ions under different conditions. The data obtained from these experiments provided valuable insights into the performance of the adsorbent and its suitability for metal ion removal applications.

$$q_t = \frac{(C_o - C_t)\,V}{m}\ mg/g \qquad (1)$$

Here's what each symbol represents:

- q_t - This represents the quantity of a substance (usually expressed in moles or grams) at a specific time point, denoted by "t".
- C_o - This is the initial concentration of the substance.
- C_t - This is the concentration of the substance at the time point "t".
- V - This represents the volume of the solution or system in which the substance is present.
- m - This represents the molar mass (usually expressed in grams per mole) of the substance.

After subjecting the metal ion solutions to a 5-minute centrifugation, the concentration of the remaining metal ions was determined using instrumental analysis (AAS). The analysis was performed dual times and the average value of this final output reading was taken for experimental purpose. Data collected from batch studies can be used to calculate metal ion removal percentages. A quantitative assessment is therefore possible to determine whether the targeted metal ions are effectively removed from the solution by adsorption. This calculation provides valuable information about the effectiveness of the adsorption process in removing the targeted metal ions from the solution. Equation 2 establishes a mass balance relationship that facilitates the calculation of the amount of metal ions retained by the AN Seaweed biochar. By assessing characteristics including the initial concentration of Cr, Ni and Zn, the equilibrium concentration following adsorption, the volume of the solution, and the mass of the adsorbent employed, this equation provides a quantitative relationship that aids in comprehending the adsorption process and determining the degree of metal ion removal (Aydına *et al*, 2021). It allows for a precise assessment of the adsorption capacity and efficiency of the adsorbent in removing metal ions from the solution.

It allows researchers to assess the efficiency and capacity of the adsorbent in capturing and retaining the targeted metal ions from the solution. By utilizing equation 2 in conjunction with the corresponding experimental data, it becomes feasible to conduct a quantitative measurement for the calculation of adsorption efficiency. This assessment allows for the determination of the degree of metal ion removal achieved by the adsorbent.

$$\%\ \text{Removal} = \left[\frac{C_o - C_e}{C_o}\right] X100 \qquad (2)$$

Here's what each symbol represents:

- % Removal: This represents the percentage of the substance that has been removed from the system.
- C_o: This is the initial concentration of the substance in the system.
- C_e: This is the concentration of the substance remaining in the system after removal or treatment.

2.5. Temperature & thermodynamic studies

The batch adsorption process was performed under various temperatures to check the metal ion uptake by AN biochar follows exothermic/endothermic. i.e., the temperature ranging from 15 - 60°C with gradual interval of 15°C. The purpose of these experiments was to investigate how the temperature affects the metal ion uptake by AN biosorbent. By comparing the adsorption efficiency at different temperatures, it is possible to analyse the thermodynamic behaviour of the adsorption process and determine whether it is exothermic (releasing heat) or endothermic (requiring heat). The initial concentrations of metal ions, AN biochar dose and solution's pH were maintained at constant range during this experimental analysis. The experimental data acquired from the batch experiments were employed to

calculate significant thermodynamic variables associated with the adsorption process. These parameters include the Gibbs free energy change (ΔG°), enthalpy change (ΔH°), and entropy change (ΔS°). By determining these thermodynamic values, it is possible to gain insights into the spontaneity (ΔG°), energy changes (ΔH°), and disorder (ΔS°) of the adsorption process. The following equations (3), (4) & (5) were employed to calculate the thermodynamic parameters:

$$K_c = \frac{C_{Ae}}{C_e} \tag{3}$$

$$\Delta G_0 = -RT\ln K_C \tag{4}$$

$$\log K_c = \frac{\Delta S^0}{2.303R} - \frac{\Delta H^0}{2.303RT} \tag{5}$$

Here's what each symbol represents:

- Kc: This represents the equilibrium constant for the chemical reaction. It is a dimensionless quantity and indicates the relative concentrations of reactants and products at equilibrium.
- CAe: This is the equilibrium concentration of species A in the reaction. It refers to the concentration of species A when the reaction has reached equilibrium.
- Ce: This is the equilibrium concentration of another species, denoted as e, in the reaction. It represents the concentration of species e when the reaction has reached equilibrium.
- ΔG°: This represents the standard Gibbs free energy change for the reaction. It is a measure of the spontaneity or thermodynamic feasibility of the reaction under standard conditions.
- R: This is the gas constant, which relates the energy scale to temperature. It has a value of approximately 8.314 J/(mol·K) or 0.008314 kJ/(mol·K).
- T: This is the temperature in Kelvin (K) at which the reaction is occurring.
- ln(Kc): This is the natural logarithm of the equilibrium constant (Kc) for the reaction.
- Log(Kc): This represents the logarithm (usually base 10) of the equilibrium constant (Kc) for the chemical reaction.
- ΔS°: This is the standard entropy change for the reaction. It represents the difference in entropy between the reactants and products at standard conditions.
- ΔH°: This is the standard enthalpy change for the reaction. It represents the changes in between products and reactants under the optimum conditions.
- R: This is the gas constant, which relates the energy scale to temperature. It has a value of approximately 8.314 J/(mol·K) or 0.008314 kJ/(mol·K).
- T: This is the temperature in Kelvin (K) at which the reaction is occurring.

2.6. Adsorption isotherm studies

2.6.1. Langmuir isotherm model

The Langmuir isotherm equation is a commonly employed mathematical model that explains adsorption phenomena, especially in cases of monolayer adsorption, wherein the adsorbate molecules primarily attach to the adsorbent surface through chemical reactions. According to the Langmuir isotherm, all sites on the adsorbent have an equivalent preference for the adsorbate. The Langmuir isotherm also relies on certain assumptions. It assumes that the processes involved are homogeneous, meaning there is only one type of adsorbate present. In this assumption, it is considered that the adsorbate molecules solely interact with a single active site on the adsorbent, and no interactions take place among the adsorbate species (Ambaye *et al*, 2021). In addition, the Langmuir isotherm makes the assumption that the surface phase formed by the adsorbate molecules is a monolayer, implying that only a single layer of adsorbate molecules is formed on the surface of the adsorbent. The linear equation of Langmuir isotherm study indicates in the following Equation 6 as follows:

$$\frac{C_e}{q_e} = \frac{1}{K.q_{max}} + \frac{C_e}{q_{max}} \tag{6}$$

Here's what each symbol represents:

- Ce: This symbolizes the equilibrium concentration of the substance in the solution or system.
- qe: This signifies the amount/quantity adsorbed on the surface at equilibrium.
- K: This is the adsorption equilibrium constant, which relates the concentration of the substance in the solution to the quantity adsorbed on the surface.
- q_{max}: amount of targeted ions uptake on the AN biochar's surface, often referred to as the maximum adsorption capacity.

2.6.2. Freundlich isotherm model

Equation 7 represents the Freundlich isotherm equation, which accounts for the possibility of multi-layer adsorption on the surface of the adsorbent.

$$\ln q_e = \ln k_f + \frac{1}{n}\ln C_e \tag{7}$$

Here's what each symbol represents:

- ln (q_e): This represents the natural logarithm of the quantity adsorbed on the surface at equilibrium.
- ln(k_f): This represents the natural logarithm of the constant and it indicates the capacity of adsorption
- (1/n): This term represents the reciprocal of the exponent "n" in the Freundlich equation, which characterizes the adsorption intensity.
- ln (C_e): This represents the natural logarithm of the equilibrium concentration of the substance in the solution or system.

2.6.3. Sips isotherm model

The Sips model isotherm analysis was employed to forecast the adsorption mechanism at extremely low concentrations. This type of isotherm model was developed by combining the above two isotherms (Langmuir & Freundlich) to examine the homogeneous sites within the adsorbent material. The Sips model isotherm characterizes the adsorption process as a monolayer adsorption, disregarding the concentration of metal ions in solutions (Khan *et al*, 2022). The corelation between the equilibrium sorption quantity ($1/q_e$) and the concentration of chromium ion solutions (C_e) at 30°C can be described by the equation 8:

$$\frac{1}{q_e} = \frac{1}{Q_{max} K_s} \left(\frac{1}{C_e} \right)^{\frac{1}{n}} + \frac{1}{Q_{max}} \quad (8)$$

where Q_{max} represents the maximum adsorption capacity, K_s is the equilibrium constant, and n is the Sips model exponent.

2.6.4. Toth isotherm model

The Toth isotherm model, known as a three-parameter isotherm, is commonly employed for solid surfaces that exhibit homogeneity. This model effectively considers the interaction and collaboration between the adsorbed pollutants, providing a comprehensive understanding of the adsorption process (Fideles *et al*, 2019). The Toth model is known for its high accuracy, particularly at low concentrations, making it a dependable approach for predicting and analysing adsorption behaviour. The natural logarithm of the ratio between the equilibrium sorption quantity (q_e) and the difference between the maximum sorption capacity (q_m) and q_e can be stated in equation 9:

$$\ln \frac{q_e}{q_m - q_e} = n \ln K_L + n \ln C_e \quad (9)$$

Here, n represents the Toth model exponent, K_L is the Toth model constant, and C_e denotes the equilibrium concentration of the adsorbate. This equation describes the relationship between these parameters in the Toth isotherm model.

2.6.5. Kinetic studies

To optimize the adsorbent material and gain a deeper understanding of the interaction between metal ions and activated Ascophyllum nodosum (AN) biosorbent, kinetic studies were undertaken. These studies utilize kinetic models to assess the effectiveness of the Ascophyllum nodosum adsorbent and the underlying mass transfer mechanisms. Kinetic models help in analysing and understanding the rate and mechanisms of adsorption, aiding in the optimization of the adsorption process (Candamano *et al*, 2022). Several kinetic models are commonly utilized to evaluate the adsorption process when employing adsorbent materials. These models include:

2.6.6. Pseudo first order study

The Lagergren kinetic model, also referred to as the first-order kinetic model, is frequently employed to assess the adsorption capacity of solid materials in both liquid and solid systems. This model assumes that the adsorption process follows a first-order rate equation, where the rate of adsorption is directly proportional to the difference between the initial concentration and the concentration at a given time (Hong *et al*, 2020). By studying the kinetics of adsorption using the Lagergren model, valuable insights can be gained regarding the rate and efficacy of the metal ions uptake. The adsorption of heavy metals by AN biochar was evaluated by comparing their initial concentration (q_e) with their equilibrium concentration (q). This approach allows for the evaluation of the extent of adsorption and provides insights into the effectiveness of the biochar as an adsorbent for heavy metal ions. At equilibrium, the total volume of heavy metal ions absorbed by the AN biochar at a given time (t) can be determined by measuring the equilibrium concentration (q_e) and the instantaneous concentration (q) was expressed in Equation 10.

$$\log(q_e - q) = \log q_e - \frac{k}{2.303} t \quad (10)$$

In this equation, log (q_e - q) represents the logarithm of the difference between the equilibrium concentration (q_e) and the instantaneous concentration (q) at a given time (t). The term log(q_e) represents the logarithm of the equilibrium concentration. The term (k/2.303) t represents the rate constant (k) multiplied by time (t) divided by a conversion factor (2.303).

2.6.7. Pseudo second order study

The whole range of adsorption process was predicted and controlled by chemisorption mechanism and the Pseudo second order study follows the above said mechanism by rate controlling step to find the rate of adsorption during earlier stages and time of reaction (Dulla *et al*, 2020). It is found to be able to predict the behaviour of adsorption for all range of concentrations. Equation 11 represents the pseudo second order linear form.

$$\frac{t}{q_t} = \frac{1}{kqe^2} + \frac{t}{q_e} \quad (11)$$

Here, kqe^2 represents the rate of adsorption, q_e denotes the equilibrium concentration, and t is the time. This equation allows for the analysis of the relationship between time and adsorbate concentration, providing insights into the adsorption process.

2.6.8. Boyd kinetic study

The rate controlling step of heavy metal adsorption by the biosorbent was determined using the Boyd kinetic model. The Boyd kinetic equation, as shown in equation 12, was used to analyse the data. The value of Di, which represents the effective diffusion coefficient, can be calculated using Equation 13 after obtaining the B values from the Boyd kinetic plots.

$$Bt = -0.4977 - \ln(1 - F) \quad (12)$$

$$B = \frac{\Pi^2 D_i}{r^2} \quad (13)$$

2.6.9. Elovich kinetic study

The Elovich kinetic study was employed to evaluate the biochar adsorbent and its interaction with gas molecules through the early phases of heavy metal ion acceptance (Khalid *et al*, 2019). This kinetic model assumes that the increase in the desorption rate is exponential with decrease in adsorbed solute and its vice versa. The linear equation representing this Elovich kinetic model can be depicted as equation 14:

$$q_t = \frac{1}{b}\ln(1+abt) \qquad (14)$$

The ability of adsorption and the constant for desorption was indicated by a & b respectively.

3. Results and discussion

3.1. SEM & EDX analysis

Figure 2(a) shows a scanning electron microscopy (SEM) image of Ascophyllum nodosum, highlighting its irregularly shaped and porous surface. In this metal ions adsorption, the surface morphology plays a significant role using the biosorbent. The Energy Dispersive X-ray (EDX) analysis, depicted in Figure 2(b), provides further insights into the elemental composition of Ascophyllum nodosum and confirms its suitability for metal ion adsorption. These analytical techniques contribute to the understanding of the surface characteristics and adsorption potential of Ascophyllum nodosum as a valuable adsorbent for heavy metal removal. The presence of such a porous structure is advantageous for effective adsorption processes. Figure 2(c) displays the EDX image of Ascophyllum nodosum, revealing the occurrence of targeted heavy metals (Cr, Ni & Zn) on the surface of the adsorbent. This image provides visual confirmation of the successful adsorption of metal ions onto the accessible surface of Ascophyllum nodosum. The functional groups present on the inner walls of the adsorbent are responsible for facilitating the adsorption process by interacting with and binding the metal ions. The surface morphology study conducted provides evidence that the metal ions are absorbed within the internal walls of the AN biochar's surface (Biswas *et al*, 2015). This finding emphasizes the effective adsorption capacity of Ascophyllum nodosum for the elimination of heavy metals.

The EDX image of the metal ion loaded adsorbent indicates the presence of carbon, oxygen, and sulphur, which are inherent components of the raw adsorbent. Figure 2(c) and (d) also reveal the detection of other metal elements/components, including calcium, silica, and chlorine, alongside the presence of chromium, nickel, and zinc ions. Treating Ascophyllum nodosum with sulfuric acid, involving the reaction with concentrated sulfuric acid, results in the formation of sulfuric esters as non-ionic functional groups. These functional groups may form complexes with cations, facilitating the adsorption of metal ions (Aswini *et al*, 2019). From the information given, it can be deduced that the utilization of a sulfuric acid solution successfully protonates the charged sites present on the surface of the adsorbent. This treatment does not appear to significantly disrupt any important functional groups present in the raw adsorbent.

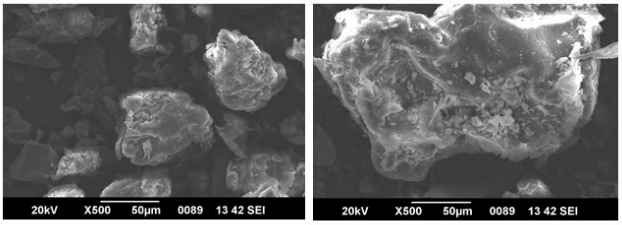

Figure 2. (a) SEM image of AN before metal ion adsorption and 2 (b) SEM image of AN after-metal ion adsorption

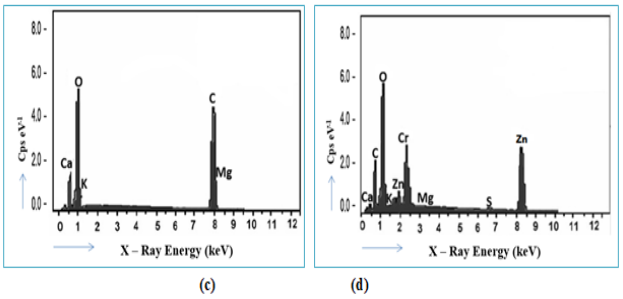

Figure 2. (c) EDX image of AN before metal ion adsorption and 2(d) EDX image of AN after-metal ion adsorption

3.2. FT-IR studies

Figure 3(a) & (b) shows the results of FTIR analysis conducted on both Ascophyllum nodosum and Ascophyllum nodosum samples loaded with Cr (VI), Ni (II), and Zn (II) metal ions. The analysis of the spectra reveals the identification of specific functional groups and their corresponding vibrational modes. The spectra were observed when the region has very high energy, a distinct peak at a wave number of 3420 cm^{-1} is observed, suggesting the existence of hydroxyl (-OH) groups. Similarly, the presence of $-CH_2$ groups is detected at 2860 cm^{-1}, suggesting the existence of methylene groups (Li *et al*, 2012). In the wave number range of 1000 cm^{-1} to 1800 cm^{-1}, various bands can be assigned to different vibrations. The peaks at 1620 cm^{-1} correspond to the vibrations of H_2O molecules, while the peaks at 1600 cm^{-1} and 1460 cm^{-1} indicate aromatic vibrations. The FT-IR analysis of Ascophyllum nodosum and metal ion loaded Ascophyllum nodosum reveals specific vibrational bands in the spectra. The bands observed at wave numbers 1380 cm^{-1} & 1400 cm^{-1} are indicative of $-CH_2$ bending vibrations, suggesting the presence of methylene groups in the analysed sample. The peak observed at 1080 cm^{-1} in the spectroscopic analysis can be attributed to the vibrations of C-O bonds. If there were aromatic vibrations resulting from C-H bending, the peak would typically appear at a wave number below 1000 cm^{-1}. The FT-IR spectra also exhibit lower frequency peaks corresponding to aromatic ring vibrations and -OH stretching vibrations, suggesting the contribution of these functional groups in the adsorption process (Pham *et al*, 2021). Moreover, the $-CH_2$ stretching vibrations disappear at 2860 cm^{-1}. The presence of active sites on the adsorbent surface can be inferred from these observations, indicating their involvement in the adsorption process.

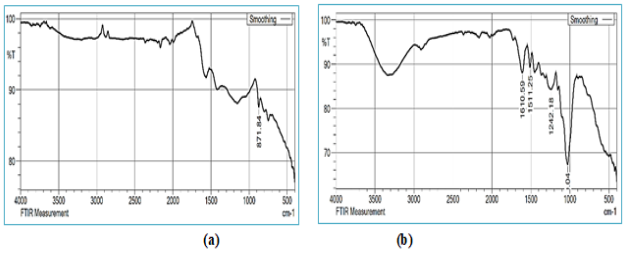

Figure 3. (a) - FTIR image of AN before metal ion adsorption and 3 (b) - FTIR image of AN after-metal ion adsorption

3.3. Effect of pH

The objective of this study was to inspect the influence of solution pH on the efficiency of heavy metal elimination, specifically Cr, Ni & Zn ions, using Ascophyllum nodosum (AN) as the biosorbent. The pH range examined in this study varied from 2.0 to 7.0. The outcomes indicate that the pH of the solution escalates, the efficiency of heavy metal elimination declines. The readings from the experiment indicated that the lowest percentage of metal ion removal occurred at pH 6.0. Figure 4a illustrates that at lower pH levels, the surface of AN biochar is covered by hydronium ions. At lower pH values, the adsorbent surface tends to acquire a positive charge. This positive charge enhances the interaction between the metal ions and the adsorbent, leading to increased adsorption efficiency. As the solution pH increases, the efficiency of metal ion removal decreases. This is attributed to the highly positive charge on the adsorbent surface, which reduces the interaction between the metal ions and the adsorbent (Homaidan *et al*, 2018). The decrease in the removal of heavy metal ions from the solution is a consequence of the reduced interaction between the metal ions and the adsorbent. Moreover, as the pH of the solution increases, the stability of the metal ions decreases. It is noteworthy that the adsorption process reaches equilibrium at pH 6.0, indicating that this pH level is critical for achieving the optimal balance between metal ion removal and adsorbent stability. The decrease in metal ion removal at higher pH values can be attributed to the formation of metal hydroxides, leading to their precipitation. The Ascophyllum nodosum powder exhibits maximum removal percentages of 83.27% for Zn (II), 87.56% for Ni (II), 93.55% for Cr (VI) and at the optimal pH.

3.4. Effect of AN biochar dose

The quantity of adsorbent employed is a vital parameter for achieving effective removal of metal ions since it directly influences the availability of active sites for adsorption. Figure 4b provides a visual representation of the effect of different quantities of AN biochar on the elimination of heavy metals. The observational findings exhibit that the greatest percentages of heavy metals removal for Cr (VI), Ni (II), and Zn (II) were attained when a dosage of 2.5 g/L of Ascophyllum nodosum was used. Specifically, the maximum removal percentages were determined to be 59.2% for Zn (II), 77.7% for Ni (II) and 93.55% for Cr (VI) at this particular dosage. Adsorbent surfaces with more active sites are said to improve the efficiency of heavy metal removal from aqueous solutions. By augmenting the dosage of the adsorbent, a greater number of active sites are provided for adsorption, resulting in higher percentages of metal ion removal. This increase in adsorbent dosage enhances the surface area available for adsorption, allowing for greater contact between the metal ions and the adsorbent, leading to improved removal efficiency (Chakraborty *et al*, 2022). However, it is worth noting that there might be an optimal dosage beyond which further increases may not significantly improve the removal efficiency.

3.5. Effect of contact time

To examine the influence of contact time on the biosorption of metal ions (Cr, Ni, and Zn), the metal ion containing solution's concentration was varied across the range of 25 to 150 mg/L. The contact time was adjusted from 10 to 120 minutes to assess the influence of different durations on the adsorption process. Figure 5(a), (b), and (c) provide graphical representations of the changes in metal ion removal as a function of different contact periods. Due to a greater number of vacant sites on the adsorbent's surface during the early stages of contact time, metal ions are rapidly removed. These vacant sites provide ample opportunities for metal ions to interact and adsorb onto the surface, leading to fast removal kinetics (Olawale *et al*, 2022). Furthermore, the heavy metallic ions were absorbed into the meso-pores of the adsorbent, which initially had more capacity for adsorption and quickly became saturated. Following an incubation period of 60 minutes, the elimination of metal ions reached a plateau, indicating that no significant change in the removal efficiency was observed beyond this point. The existence of antagonistic forces among the adsorbate molecules and the solid surface can be attributed to the inhibition of cohesive adsorption interactions, leading to a hindered further adsorption process (Bazrafshan *et al*, 2017).

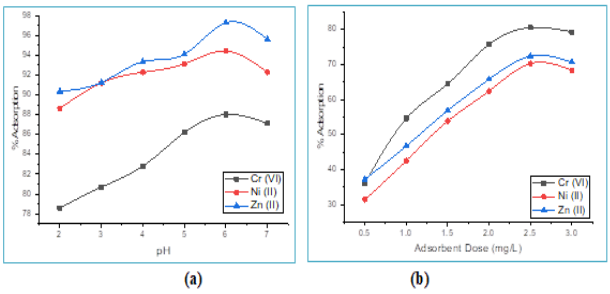

Figure 4. (a) – Impact of pH and 4 (b) Impact of adsorbent dose – for metal ion removal using AN biosorbent

These repulsive forces counterbalance the attractive forces driving adsorption, leading to a saturation point where the removal rate remains constant. The transfer of masses between liquid and solid phases has been drops with the rises in contact time. This can be attributed to the fact that as the contact time rises, the metal ions need to traverse longer distances and penetrate deeper into the pores of the adsorbent. This process demands more energy and strength as the metal ions encounter greater resistance within the adsorbent's porous structure. As a result, the mass transfer rate gradually diminishes over time, indicating that the adsorption process becomes

slower and requires more effort for the metal ions to access and retain the adsorption sites within the adsorbent (Jinzhen *et al*, 2022). Consequently, the adsorption process slows down during the later stages of contact time. Overall, the optimum contact time for maximum removal of metal ions was found to be around 60 minutes in the experimental conditions.

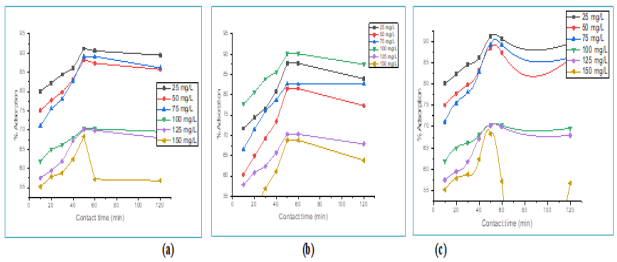

Figure 5. Effect of contact time for (a) Cr, (b) Ni & (c) Zn metal ion adsorption using AN biosorbent

3.6. Impact of temperature

By conducting experiments at different temperatures from 15 to 60 degrees Celsius, this study investigated the effect of temperature on metal ion adsorption. As the temperature rises, the metal ions uptake exhibited a gradual improvement in efficiency, eventually reaching a steady state at the optimal temperature of 45 degrees Celsius. This suggests that higher temperatures enhance the adsorption efficiency of the adsorbents. However, beyond this temperature, the efficiency started to decrease. The observed trend can be ascribed to the higher desorption rate of metal ions from the adsorbent surface at elevated temperatures, leading to a decrease overall adsorption capacity (Su *et al*, 2021). Figure 6a visually represents the ability of AN biochar adsorbent for the metal ion removal at various temperature levels, spanning from 15 to 60 degrees Celsius. The results show that the efficiency increases as the temperature rises until it reaches the optimum temperature of 45 degrees Celsius. However, beyond this point, the efficiency starts to decline. Understanding the relationship between temperature and adsorption efficiency is crucial for comprehending the thermodynamics of metal ion uptake and optimizing the conditions to achieve maximum adsorption capacity.

3.7. Effect of metal ion concentrations

By analysing the data depicted in Figure 6b, it is evident that there is a gradual decline in the removal of heavy metals as the concentration increases. The metal ion concentrations ranging from 25 to 150 mg/L was taken and the impact of efficiency of metal ion uptake has been examined. The active sites present on the AN biochar's surface was reached to the saturation level with increase in metal ion concentrations. Consequently, the available capacity for adsorption decreases, resulting in a decline in the percentage of adsorption. This phenomenon indicates that at higher concentrations of metal ions, the adsorbent's ability to adsorb further ions becomes limited (Foday *et al*, 2021). For Cr (VI), the adsorption percentage decreases from 98.63% to 64.26%, for Ni (II) it decreases from 89.27% to 68.92%, and for Zn (II) it decreases from 82.39% to 68.82%. The decrease in the adsorption percentage by the rise in the concentration of metal ions indicates that the adsorbent material has not yet reached its saturation threshold. This indicates that there are still unoccupied adsorption sites on the surface of the adsorbent, which have the potential to bind and capture additional metal ions (Vieites *et al*, 2022). The uniform decrease in adsorption amount with increasing metal ion concentration further supports this observation. The findings additionally demonstrate a significant distinction in the adsorption characteristics of Ascophyllum nodosum when exposed to single metal ions versus multi-metal ions.

When single metal ions are adsorbed, a tendency towards higher adsorption efficiency is observed in comparison to multi-metal ion systems. This discrepancy can be primarily attributed to the presence of a greater quantity of specific adsorption sites that are specifically tailored to bind with the particular metal ion of interest, leading to the heightened adsorption efficiency observed in single metal ion adsorption scenarios (Ibuot *et al*, 2017). When only one metal ion is present in the solution, the adsorbent can allocate more of its active sites to adsorb and remove that specific metal ion, leading to higher adsorption efficiency. Nonetheless, in multi-metal ion systems, the simultaneous presence of multiple metal ions introduces a competitive dynamic for the available adsorption sites, leading to diminished adsorption efficiency for each individual metal ion. When multi-metal ions are present at higher concentrations, there is a heightened competition among the metal ions to occupy the limited adsorption sites (Chugh *et al*, 2022).

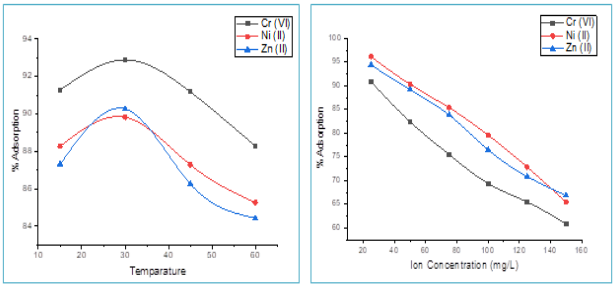

Figure 6. (a) – Impact of Temperature & 6 (b) Impact of metal ion concentration for the adsorption of metal ions

The findings indicate that Cr (VI) has a higher affinity and competitive advantage over Ni (II) and Zn (II) on the adsorbent surface, leading to its ability to displace and replace these ions in the adsorption process. This can be attributed to factors such as the higher atomic weight and paramagnetic nature of Cr (VI), its high reduction potential, and the lower hydration energy and ionic radius of Cr (VI) compared to Ni (II) and Zn (II). Overall, the adsorbent exhibits higher performance for the removal of Cr compared to other metal ions due to several factors that contribute to its easier adsorption onto the adsorbent surface (Kharel *et al*, 2023). These factors may include the inherent attraction or specific binding capacity of the adsorbent for Cr, the presence of active sites on the adsorbent surface that are particularly effective in

capturing metal ions, and the favourable chemical interactions between Cr and the functional groups present on the adsorbent. Additionally, the physicochemical properties of Cr, such as its high charge density and oxidation state, may enhance its adsorption affinity towards the adsorbent material. As a result, the adsorbent demonstrates higher removal efficiency for Cr compared to other metal ions in the studied system.

3.8. Adsorption isotherm studies

3.8.1. Langmuir adsorption isotherm

The linear plots of Langmuir isotherm study were shown in Figure 7a and it indicates the relationship between capacity of adsorption and concentration during the equilibrium time. The plotted data illustrate the adsorption behaviour of specific metal ions using Ascophyllum nodosum as the adsorbent. This model describes the adsorption process, which adopts that metal ion uptake occurs in a monolayer mode on the AN biochar's surface. The metal ion uptake by the biosorbent follows monolayer mechanism and this the basic assumption of Langmuir model, wherein there are a limited number of identical and energetically equivalent active sites existing on the AN biochar's surface (Mustapha *et al*, 2019).

The plots demonstrate a linear correlation, suggesting that the adsorption process adheres to the Langmuir model, and the adsorbent surface possesses a limited adsorption capacity for the metal ions. The Langmuir isotherm plots provide insights into the maximum adsorption capacity (q_e max) and the equilibrium constant (K) for each metal ion adsorption onto Ascophyllum nodosum. The Langmuir isotherm can provide insights into the adsorption capacity and affinity of an adsorbent for a specific adsorbate (Shafiq *et al*, 2021). Table 2 presents the Langmuir isotherm constants obtained from the isotherm plots for metal ion adsorption using Ascophyllum nodosum at a temperature of 30°C. The Langmuir adsorption constant (k), which signifies the affinity of the adsorbate for the adsorbent surface, is provided for each metal ion. Additionally, the maximum adsorption capacity (q_{max}), which corresponds to the highest amount of metal ions that can be adsorbed per unit weight of the adsorbent, is listed. In addition, the regression coefficient (R^2) is included in Table 2, which indicates the goodness of fit of the Langmuir isotherm model to the experimental data. The Langmuir isotherm constants, along with the R^2 value, provide valuable insights into the adsorption characteristics of targeted metal ions onto Ascophyllum nodosum at the given temperature. The regression coefficient (R^2) values obtained for all three heavy metallic ions with a concentration of 100 mg/L are less than 1, indicating that the adsorption process is favourable. The correlation between predicted and experimental values was good by referring the R^2 values of each plot and it indicates the suitability of Langmuir isotherm model. This suggests that the adsorption of metal ions onto Ascophyllum nodosum follows the behaviour predicted by the Langmuir isotherm.

3.8.2. Freundlich adsorption isotherm

Figure 7b displays the graphical representation of the equilibrium adsorption capacity (ln q_e) plotted against the equilibrium concentration (ln Ce) for the removal of heavy metal ions using Ascophyllum nodosum as the adsorbent. The plots exhibit a linear trend, suggesting that the adsorption process can be effectively described by the Langmuir isotherm model. The observed linearity in the plots specifies that the uptake of these metallic ions onto Ascophyllum nodosum follows the Langmuir adsorption mechanism. According to this model, the adsorbent surface possesses a fixed adsorption capacity and exhibits a specific affinity for the metal ions being adsorbed (Bayuo *et al*, 2023). The Freundlich constants of K_f and n were obtained using the linear plots of this model. The Freundlich isotherm is an experiential model that describes heterogeneous adsorption surfaces and assumes multilayer adsorption with varying adsorption energies. The Freundlich constants K_f and n, as well as the regression coefficient (R^2), were calculated from the ln qe versus ln Ce plots and are listed in Table 2 at a temperature of 30°C. The interpretation provided is correct. The extent of the non-linear relationship between adsorption and the concentration of metallic ions are represented by the value of n in the adsorption isotherm equations, such as the Freundlich equation. A value of n greater than 1 suggests a physically oriented adsorption process, where the adsorbate exhibits a stronger attraction to the surface of the adsorbent (Condurache *et al*, 2022).

In this case, the obtained standards of targeted metal ions adsorption onto Ascophyllum nodosum (2.398, 1.306, and 2.547, respectively) are all greater than 1. The readings determines that the heavy metallic ions uptake process is favourable and that the adsorbate ions have a higher affinity for the Ascophyllum nodosum surface. Furthermore, the comparison of R^2 values derived from the Langmuir and Freundlich isotherm models is important in determining the best-fit model for the adsorption process. In this study, the higher R^2 values obtained for the Langmuir isotherm model compared to the Freundlich isotherm model suggest that the Langmuir model provides a better fit for the adsorption of Cr (VI), Ni (II), and Zn (II) ions onto Ascophyllum nodosum. The evidence suggests that the adsorption process conforms to a monolayer adsorption mechanism characterized by a limited number of adsorption sites. The obtained regression coefficient (R^2) values suggest that the Langmuir isotherm model provides a more accurate representation of the adsorption of metal ions using Ascophyllum nodosum related to the Freundlich isotherm model. The higher R^2 values obtained for the Langmuir isotherm model indicate a stronger agreement between the results during experiment and the model, suggesting the single layer adsorption mechanism with a limited number of adsorption sites (Elewa *et al*, 2023). This implies that the metal ions are adsorbed onto the Ascophyllum nodosum surface in a uniform and specific manner. Overall, the observations suggest that the

adsorption of metal ions onto Ascophyllum nodosum occurs through a heterogeneous and monolayer adsorption mechanism, where the metal ions form a single layer on the adsorbent surface. The Langmuir isotherm model provides a suitable representation of this adsorption process.

3.8.3. Sips isotherm study

Figure 7c represents the Sips model isotherm plot which shows the applicability of isothermal model in biosorption process. By analysing the heterogeneity factor (n) value derived from the sips isothermal plots of the model, it was possible to discern whether the adsorption process exhibited homogeneity or heterogeneity (Wang *et al*, 2023). The plots of Sips model studies and its regression (R^2) values were found to be high which indicates the suitability of this model. The 'n' value, ranging from 0 to 1, was used to determine whether the Langmuir or Freundlich isotherm fit was appropriate. If n > 1, the process fitted with Freundlich isotherm fit.

3.8.4. Toth isotherm study

The Toth isotherm model was used to identify the heterogeneous solid surface, based on its constant values. The constants (Q_{max}, b_T & n_T) were obtained and listed in Table 2 with the help of isothermal plots shown if Figure 7d. This three-parameter model is known for providing high accuracy of isotherm fitting. The interaction between the adsorbent surfaces and heavy metal pollutants were analysed using this model, but the plots provide very low regression (R^2<0.95) with respect to the biosorption process and it did not fit well with the biosorption process. If the adsorption mechanism was not properly fitted with the Langmuir isotherm mode, the Toth isotherm may be used to fit the experimental data (Pereira *et al*, 2023). In this experimental study, the Langmuir model was fitted well with the biosorption of metal ions using AN biochar, indicating that the Toth isotherm study is not necessary to check the favourable fitting of the adsorption process.

Table 2. Constants of isothermal model for the adsorption of heavy metal ions using AN biochar seaweed

S. No.	Model	Parameters	Calculated values		
			Cr (VI)	Ni (II)	Zn (II)
1.	Langmuir	q_{max}	10.472	8.124	9.608
		K_L	0.436	0.385	0.510
		R^2	0.9982	0.9866	0.9683
2.	Freundlich	K_f	2.398	1.306	2.547
		n	3.102	2.823	3.049
		R^2	0.926	0.9858	0.9778
3.	Sips	K_S	11.869	10.735	12.263
		β_S	1.5823	2.0082	1.6730
		a_S	0.2316	0.2631	0.2225
		R^2	0.9548	0.9647	0.9732
4.	Toth	Q_{max}	26.983	25.473	24.800
		b_T	0.412	0.309	0.524
		n_T	0.690	0.737	0.610
		R^2	0.926	0.905	0.912

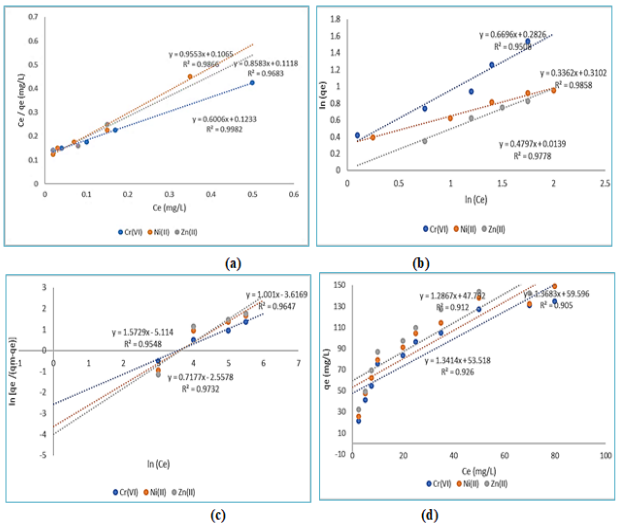

Figure 7. (a) Langmuir, (b) Freundlich, (c) Sips & (d) Toth – isotherm plots for the metal ion adsorption using AN biochar seaweed

3.8.5. Kinetic studies

3.8.6. Pseudo – first order study

The adsorption process of metal ions is often described using the pseudo-first-order reaction model or Lagergren model, which is a widely used kinetic model. Figures 8(a), (b) & (c) for Cr, Ni & Zn metal ions were used to evaluate the rate constant and regression values of first order kinetic studies. The calculated values for the pseudo first order kinetic model have been provided in Table 3 with variations in metal ion concentrations. The high correlation coefficients (R^2) obtained from the pseudo-first-order kinetics model demonstrate a robust agreement between the experimental data and the model predictions. The rate constant 'k' represents the rate of adsorption and provides insights into the adsorption kinetics. Higher values of 'k' indicate faster adsorption rates, while lower values suggest slower kinetics. The goodness of fit between Lagergren model and experimental data was assessed based on the quantitative

measures of R^2 values. These regression values approached to 1, suggests a stronger relationship between first order kinetics and the process of metal ion adsorption. These results suggest the Lagergren kinetic model can successfully define the adsorption kinetics of metal ions in the given concentration range, and the calculated rate constants and correlation coefficients provide quantitative measures of the adsorption rate and the goodness of fit for the model (Edet *et al*, 2020). Hence, the adsorption kinetics of metal ions adhere to Lagergren model suggests that the adsorption rate relies on both the active sites availability on the biosorbent and metal ion concentrations. This finding infers that the metal ion uptake is ruled by the contact between the metal ions and the adsorbent surface, where the availability of adsorption sites and the concentration of the metal ions play crucial roles.

3.8.7. Pseudo – second order kinetic model

The pseudo-second-order kinetic model offers an alternative approach to describe the sorption kinetics in the adsorption process, taking into account factors such as adsorbent capacity and the concentration of the adsorbate. In this model, the plot of t/q versus time 't' is analysed for different adsorbate concentrations. Figure8 (d), (e) & (f) displays the kinetics plots of t/q versus time 't' for diverse metal ions at several adsorbate concentrations. These plots provide insights into the adsorption kinetics and allow for the determination of the appropriate kinetic model.

Table 3 presents the computed correlation coefficients (R^2) and rate constant (k) values obtained from the kinetics plots. The correlation coefficient, which measures the degree of contract between the investigational data and this kinetic model, is indicative of the model's goodness of fit. A higher correlation coefficient value, closer to 1, signifies a stronger agreement between the model and the experimental data. After careful observations and analysis, it can be concluded that the adsorption process of the targeted metal ions, when using Ascophyllum nodosum, is best described by the pseudo-second-order kinetic model. This conclusion is supported by the high correlation coefficients (R^2) obtained, indicating a solid contract between the investigational data and forecast this kinetic model. The utilization of the pseudo-second-order kinetic model yields a more accurate description of the adsorption kinetics, indicating that the adsorption of metallic ions onto Ascophyllum nodosum follows a chemisorption mechanism (Estrada *et al*, 2021). This suggests that the adsorption process involves electron sharing or exchange between the adsorbent and the metal ions, indicating a stronger and more irreversible bonding between the adsorbent surface and the adsorbate. The experimental data indicates that the pseudo-second order kinetic model provides a superior fit compared to the pseudo-first order model. This is evident from the larger correlation coefficient (R^2) values and the smaller discrepancies between the measured equilibrium adsorption capacity (q_e) and the experimental q_e values. These readings specify that the pseudo-second-order model is more appropriate for studying the adsorption of metal ions using Ascophyllum nodosum as the adsorbent. The superiority of the pseudo-second-order model suggests that the adsorption process is primarily governed by chemisorption, involving strong chemical interactions between the adsorbent surface and the metallic ions (Azizian *et al*, 2021). The pseudo-first-order model, on the other hand, assumes a simple physical adsorption process and may not adequately capture the complexity of the adsorption mechanism. By considering the higher R^2 values, the contract between calculated and experimental q_e values was gradually increased and this study concluded that the second order adsorption kinetic model is most suitable to study the kinetics of adsorption using AN biochar.

3.8.8. Elovich kinetic model

Figure 9(a), (b) & (c) for targeted metal ions (Cr, Ni & Zn) was made by plotting q_t versus ln(t) which was used to evaluate the Elovich kinetic model in this adsorption process. The regression values of this model were found to be low compared with the second order kinetic studies (By referring Table 3). The lower R^2 values derived from the Elovich kinetic model suggest that it may not provide a suitable fit to the empirical evidence concerning the adsorption of targeted heavy metal ions by means of Ascophyllum nodosum as the adsorbent. This suggests that the assumption of a chemisorption process with a linear relationship between qt and ln(t) may not accurately describe the adsorption kinetics in this particular case. Therefore, based on the lower R^2 values obtained from the Elovich kinetic model compared to the pseudo-second-order kinetic model, it is recommended to prioritize the use of the pseudo-second-order model for studying the adsorption kinetics of metal ions onto Ascophyllum nodosum in this study. The Elovich model is commonly used to describe the kinetics of adsorption processes involving heterogeneous adsorbents (Aguiar *et al*, 2022). While the R^2 values may be lower compared to the pseudo-second-order model, the Elovich model can provide valuable insights into the adsorption behaviour on the heterogeneous surface of Ascophyllum nodosum.

3.8.9. Boyd Kinetic model

Figure 9(d), (e) & (f) presents the plots of B_t versus t, illustrating the removal of targeted pollutants (Cr, Ni & Zn) utilizing Ascophyllum nodosum at different concentrations. The plots exhibit a circular shape that does not intersect the source. Based on this observation, it can be inferred that the rate-determining step in the adsorption process is not governed by intra-particle diffusion (Leon *et al*, 2022). The Bt versus t plots are commonly used to examine the role of intra-particle diffusion in the metal ion removal techniques. Linear plots of Bt versus t that pass through the origin indicate that intra-particle diffusion is the rate-controlling step in the adsorption process. Conversely, when the plots exhibit a circular shape and do not pass through the origin, it indicates that external or film diffusion is the primary mechanism influencing the adsorption process (Al-Harby *et al*, 2021). Table 3 provides the calculated values of the diffusion coefficient (Di) and the intercept (B) obtained

from the Bt versus t plots, along with the corresponding regression coefficient (R^2) values. The obtained values of the regression and rate constants provide additional evidence for the importance of external or film diffusion in the adsorption process of metal ions onto Ascophyllum nodosum.

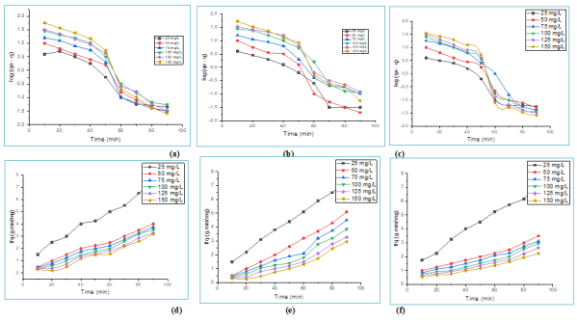

Figure 8. Pseudo plots for (a), (b) & (c) First order and (d), (e) & (f) – Second order of Cr, Ni& Zn metal ion adsorption using AN biochar

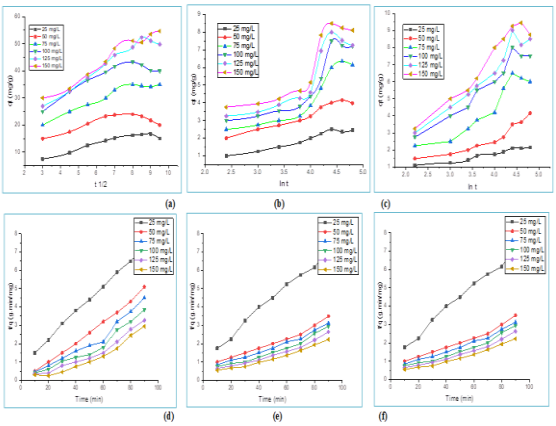

Figure 9. (a), (b) & (c) – Elovich and (d), (e) & (f) – Boyd - kinetic plots of Cr, Ni& Zn metal ion adsorption using AN biochar

Table 3. Kinetic constants for metal ions adsorption

S.No.	Type of metal	Conc.(mg/L)	Pseudo First order			Pseudo Second order				Elovich			Boyd		
			K (min^{-1})	$q_{e,}$ cal (mg/g)	R^2	K (g/mg.min)X 10^{-3}	q_e,cal (mg/g)	h (mg/g.min)	R^2	a (mg/g. min)	b (g/mg)	R^2	B	D_i(x 10^{-3} m^2/s)	R^2
1.	Cr (VI)	25	0.034	2.64	0.95	16.69	2.15	0.10	0.96	0.244	1.55	0.94	0.034	5.472	0.915
2.		50	0.043	7.02	0.93	5.73	5.19	0.18	0.98	0.988	0.74	0.93	0.044	7.340	0.973
3.		75	0.041	10.00	0.93	3.34	8.30	0.22	0.98	0.978	0.55	0.92	0.043	7.621	0.963
4.		100	0.039	11.36	0.94	5.07	10.75	0.26	0.98	0.948	0.44	0.95	0.039	6.856	0.914
5.		125	0.048	17.47	0.92	2.00	12.91	0.29	0.97	0.977	0.35	0.92	0.049	8.725	0.982
6.		150	0.045	19.43	0.93	3.12	13.82	0.30	0.96	0.934	0.26	0.92	0.045	7.452	0.952
7.	Ni (II)	25	0.046	3.68	0.91	12.62	2.70	0.10	0.97	0.263	1.16	0.91	0.046	7.678	0.943
8.		50	0.041	6.54	0.93	5.32	5.47	0.12	0.98	0.328	0.81	0.94	0.041	6.294	0.983
9.		75	0.043	9.95	0.92	3.56	8.60	0.23	0.98	0.541	0.65	0.93	0.045	7.959	0.924
10.		100	0.046	12.38	0.94	2.77	10.10	0.28	0.97	0.611	0.47	0.92	0.046	7.678	0.983
11.		125	0.052	20.55	0.92	2.30	11.56	0.31	0.98	0.618	0.31	0.90	0.053	8.590	0.941
12.		150	0.050	25.48	0.94	2.65	12.73	0.33	0.96	0.596	0.20	0.92	0.055	8.972	0.922
13.	Zn (II)	25	0.039	2.84	0.95	15.43	2.14	0.09	0.96	0.230	1.63	0.94	0.037	6.428	0.993
14.		50	0.032	6.51	0.93	5.31	5.55	0.15	0.99	0.323	0.87	0.96	0.041	6.492	0.939
15.		75	0.041	10.40	0.91	3.64	7.74	0.21	0.97	0.484	0.65	0.94	0.046	7.687	0.920
16.		100	0.044	13.27	0.95	2.86	9.40	0.27	0.98	0.572	0.46	0.93	0.050	8.344	0.942
17.		125	0.044	18.35	0.94	1.35	12.64	0.23	0.98	0.652	0.36	0.92	0.049	8.725	0.941
18.		150	0.051	23.47	0.95	1.11	15.23	0.25	0.95	0.549	0.25	0.91	0.045	8.921	0.955

3.8.10. Impact of temperature and thermodynamic studies

The results obtained at different temperatures clearly demonstrate that temperature plays a crucial role in the utilization of Ascophyllum nodosum for the adsorption of metallic ions. The greatest reduction in metallic ions was observed at 20°C, and as the temperature rose, the efficacy of metallic ion removal gradually declined and represented in Figure 10a, b & c for Cr, Ni & Zn heavy metals respectively. The adsorption activity on the AN biochar's surface got reduced with increase in temperature decreases the efficiency. Additionally, the decrease in metal ion removal as the temperature increases indicates the exothermic nature of the adsorption process. Based on this observation, it can be inferred that the adsorption of metal ions onto Ascophyllum nodosum is an exothermic process, resulting in the release of heat (Hasani *et al*, 2022). The decrease in surface activity at higher temperatures may be attributed to factors such as desorption or alterations in the surface chemistry of the adsorbent.

The thermodynamic properties, including the change in enthalpy (ΔHo), change in free energy (ΔGo), and change in entropy (ΔSo), were determined by plotting the natural logarithm of the equilibrium constant (log Kc) against the inverse of temperature (1/T). Figure 10 (d), (e) & (f) represented the thermodynamic plots for targeted metal ions in several concentration levels. Negative ΔGo values specify that the metal ion uptake is spontaneous; while positive ΔHo values suggest that the adsorption reaction is endothermic, requiring the input of heat (Adnan *et al*, 2022). The rise in entropy at the solid/liquid boundary indicates the positive ΔSo values. Also, the Positive ΔSo

values observed during the binding of metallic ions to Ascophyllum nodosum powder in an aqueous medium indicate an increase in system disorder or randomness as the metallic ions are adsorbed onto the surface of the adsorbent. This finding specifies that the metal ion uptake is thermodynamically favourable and driven by an increase in entropy (Yu *et al*, 2020). Additionally, the exothermic nature of the adsorption process indicates that heat is released during the adsorption of metal ions using Ascophyllum nodosum. Temperature is a crucial factor that impacts the efficiency of the adsorption process. Thermodynamic parameters provide valuable information about the energy changes and feasibility of the adsorption process. The thermodynamic plots, as presented in Table 4, reveal that the calculated values support the spontaneous nature of the metal ion adsorption process.

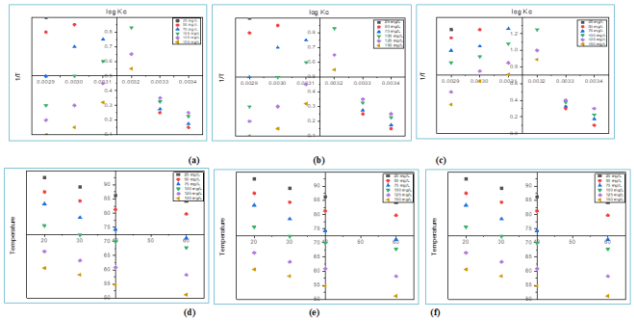

Figure 10. (a), (b) & (c) – Thermodynamic plots and (d), (e) & (f) – Temperature effect plots for targeted metal ions (Cr, Ni & Zn) adsorption using AN biochar seaweed

Table 4. Thermodynamic constants of targeted metals in various ion concentrations

Initial concentration of Cr(VI) ions (mg/L)	Enthalpy (ΔH°)KJ mol^{-1}	Entropy(ΔS°)J mol^{-1}	Gibbs Energy (ΔG_o) kJ mol^{-1}			
			15°C	30°C	45°C	60°C
25	82.284	190.203	-16.390	-11.329	-10.590	-8.466
50	39.249	97.042	-11.812	-9.536	-8.389	-7.125
75	24.393	48.993	-9.485	-8.420	-7.413	-6.002
100	15.821	31.417	-6.030	-6.959	-5.955	-4.682
125	11.299	29.055	-4.112	-4.067	-3.698	-3.011
150	9.205	24.273	-2.902	-2.236	-2.070	-2.212
Initial concentration of Ni(II) ions (mg/L)						
25	75.707	170.506	-13.495	-11.663	-9.542	-8.345
50	42.557	85.237	-11.403	-10.485	-8.632	-7.432
75	25.208	38.994	-9.570	-8.699	-7.907	-6.982
100	17.033	20.340	-7.884	-6.128	-5.473	-4.438
125	12.473	15.219	-5.358	-4.691	-3.756	-3.034
150	8.782	9.506	-4.317	-3.260	-2.967	-2.348
Initial concentration of Zn(II) ions (mg/L)						
25	80.459	173.908	-11.368	-9.657	-8.355	-6.730
50	40.379	80.447	-9.345	-8.674	-6.646	-5.544
75	25.502	45.303	-8.674	-6.396	-5.873	-4.753
100	11.336	23.229	-7.290	-5.877	-4.387	-3.542
125	8.401	11.560	-6.782	-4.575	-3.763	-3.029
150	6.114	7.040	-4.987	-3.659	-2.764	-2.426

3.8.11. Desorption studies

For the reusability studies, a quantity of 25 mg of targeted metal ions (Cr, Ni & Zn) loaded AN biosorbent was taken. Before reuse, the rice straw biosorbent underwent agitation in 50 mL of HCl solution for 1 hour to facilitate regeneration. The adsorbent was then rinsed twice with distilled water to desorb the adsorbed metal ions. Desorption studies were conducted using concentrated hydrochloric acid with a normality range of 0.1 to 0.4 to recover the spent adsorbate from the aqueous solutions. Figure 11(a) depicts the rate of desorption of metal ions by adding HCl. During the initial stages of the desorption process, the recovery of metal ions was rapid and increased proportionally with the concentration of hydrochloric acid. However, as the desorption process progressed, the desorption rate eventually reached saturation upon the addition of 0.3N hydrochloric acid to the solution. Further increase in hydrochloric acid concentration led to a reduction in the desorption rate, indicating that the equilibrium level had been attained. The exhausted AN biosorbent and its releasing capacity exhibit a direct proportional relationship with the desorption rate. As a result, the desorption rate decreases with an increase in concentration. To evaluate the performance of the adsorbent, multiple cycles of analysis were conducted. Referring to Figure 11(b), it can be observed that during the first cycle of regeneration, the recovery of metal ions was high. However, as the number of cycles increased, the amount of recovery rate gradually decreased.

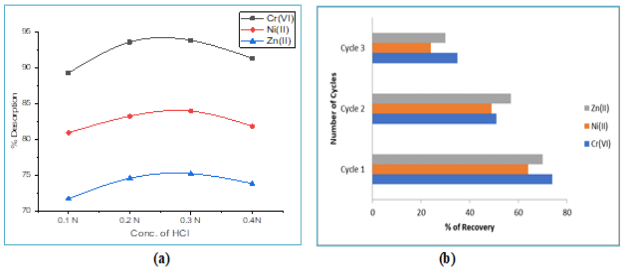

Figure 11. (a) Desorption and (b) Regeneration study plots for the metal ions removal

4. Conclusion

The Ascophyllum nodosum biosorbent and its ability to remove the chromium and lead metal ions present in the wastewater have been examined by batch mode of adsorption studies. The biosorbent was prepared through chemical synthesis and subsequently activated by the addition of concentrated sulfuric acid. The results revealed significant removal rates, with percentage of 93.55(Cr(VI)), 87.56(Ni(II)), and 83.27(Zn(II)) metal ions successfully eliminated from the synthetic solutions. These high removal percentages were achieved under optimal conditions, including a pH value of 6.0, a biosorbent dose of 2.5 g/L, an initial ion concentration of 25 mg/L, and a contact time of 50 minutes. All experimental analyses were conducted at room temperature, specifically 25°C. The isothermal studies using Langmuir, Freundlich, and Sips models provided evidence supporting a multilayer adsorption process with a heterogeneous nature. Additionally, the pseudo first-order, pseudo second-order, and Boyd kinetic studies confirmed that the uptake of metal ions by the Ascophyllum nodosum adsorbent followed a chemical adsorption process. These findings contribute to a comprehensive understanding of the adsorption behaviour and mechanism of the rice straw adsorbent in relation to metal ion removal.

References

Aguiar A.B.S., Costa J.M., Santos G.E., Sancinetti G.P., Rodriguez R.P. (2022). Removal of Metals by Biomass Derived Adsorbent in Its Granular and Powdered Forms: Adsorption Capacity and Kinetics Analysis. *Sustainable Chemistry* **3**, 535–550. https://doi.org/10.3390/suschem3040033

Al – Homaidan A.A., Al – Qahtani H.S., Al- Ghanayem A.A., Ameen F. and Ibraheem I.B. (2018). Potential use of green algae as a biosorbent for hexavalent chromium removal from aqueous solutions, *Saudi Journal of Biological Sciences*, **25** (8), 1733–1738. https://doi.org/10.1016/j.sjbs.2018.07.011

Al-Harby N.F., Albahly E.F. and Mohamed N.A. (2021). Kinetics, Isotherm and Thermodynamic Studies for Efficient Adsorption of Congo Red Dye from Aqueous Solution onto Novel Cyanoguanidine-Modified Chitosan Adsorbent. *Polymers*, **13**, 4446. https://doi.org/10.3390/polym13244446

Ambaye T.G., Vaccari M., Hullebusch E.D.V., Amrane A. and Rtimi S. (2021). Mechanisms and adsorption capacities of biochar for the removal of organic and inorganic pollutants from industrial wastewater, *International Journal of Environmental Science and Technology*, **18**, 3273–3294. https://doi.org/10.1007/s13762-020-03060-w

Aswini K. and Jaishankar V. (2019). Adsorption treatment of heavy metal removal from simulated wastewater using rice husk activated carbon and its polyvinylpyrrolidoone composite as an adsorbent. *Journal of Water and Environmental Sciences*, **3**, 460–470. https://revues.imist.ma/index.php/jwes/article/view/12465/12658

Aydına S., Nura H.M., Traorea A.M., Yıldırımb E. and Emik S. (2021). Fixed bed column adsorption of vanadium from water using amino-functional polymeric adsorbent, *Desalination and Water Treatment*, **209**, 280–288. 10.5004/dwt.2021.26493

Azizian S. and Eris S. (2021). Adsorption isotherms and kinetics. *Interface Science and Technology*, **33**, 445–509. https://doi.org/10.1016/B978-0-12-818805-7.00011-4

Bayuo J., Rwiza M.J., Sillanpää M. and Mtei K.M. (2023). Removal of heavy metals from binary and multicomponent adsorption systems using various adsorbents – a systematic review. *Advanced*, 13, 13052–13093. https://doi.org/10.1039/D3RA01660A

Bazrafshan E., Sobhanikia M., Mostafapour F.K., Kamani H. and Balarak D. (2017). Chromium biosorption from aqueous environments by mucilaginous seeds of Cydonia oblonga: Kinetic and thermodynamic studies, *Global Nest Journal*, **19** (2), 269 – 277. https://doi.org/10.30955/gnj.001708

Bich Ngoc Pham, Jin-Kyu Kang, Chang-Gu Lee and Seong-Jik Park. (2021). Removal of Heavy Metals (Cd^{2+}, Cu^{2+}, Ni^{2+}, Pb^{2+}) from Aqueous Solution Using Hizikia fusiformis as an Algae-Based Bioadsorbent, *Applied Sciences*, **11**, 8604. https://doi.org/10.3390/app11188604

Biswas S. and Mishra U. (2015). Continious fixed bed column study and adsorption modeling: removal of lead ion from aqueous solution by charcoal originated from chemical carbonization of rubber wood sawdust. *Journal of chemistry* ID: 907379. Doi: https://doi.org/10.1155/2015/907379.

Blanco-Vieites M., Suárez-Montes D., Delgado F., Álvarez-Gil M., Hernández Battez A., Rodríguez E. (2022). Removal of heavy metals and hydrocarbons by microalgae from wastewater in the steel industry. *Algal Research*, **64**, 102700. https://doi.org/10.1016/j.algal.2022.102700

Candamano S., Policicchio A., Conte G., Abarca R., Algieri C., Chakraborty S., Curcio S., Calabrò V., Crea F. and Agostinobc R.G. (2022). Preparation of foamed and unfoamed geopolymer/NaX zeolite/activated carbon composites for CO_2 adsorption, *Journal of Cleaner Production*, **330**, 129843. https://doi.org/10.1016/j.jclepro.2021.129843

Chakraborty R., Asthana A., Singh A.K., Jain B. and usan A.B.H. (2022). Adsorption of heavy metal ions by various low-cost adsorbents: a review, *International Journal of Environmental Analytical Chemistry*, **102** (2), 342–349. https://doi.org/10.1080/03067319.2020.1722811

Chugh M., Kumar L., Shah M.P., Navneeta Bharadvaja. (2022). Algal Bioremediation of heavy metals: An insight into removal mechanisms, recovery of by-products, challenges, and future opportunities. *Energy Nexus*, **7**, 100129. https://doi.org/10.1016/j.nexus.2022.100129

Condurache B.C., Cojocaru C., Samoila P., Cosmulescu S.F., Predeanu G., Enache A.C., Harabagiu V. (2022). Oxidized Biomass and Its Usage as Adsorbent for Removal of Heavy

Metal Ions from Aqueous Solutions. *Molecules* **27**, 6119. https://doi.org/10.3390/molecules27186119

Cordova Estrada A.K., Cordova Lozano F., and Lara Díaz R.A. (2021). Thermodynamics and Kinetic Studies for the Adsorption Process of Methyl Orange by Magnetic Activated Carbons. Air, *Soil and Water Research*, **14**, 1–11. https://doi.org/10.1177/11786221211013336

Dulla J.B., Tamana M.R., Boddu S., Pulipati K.and Srirama K. (2020). Biosorption of copper (II) onto spent biomass of Gelidiella acerosa (brown marine algae): optimization and kinetic studies, *Applied Water Science*, **10** (56). https://doi.org/10.1007/s13201-019-1125-3

Edet U.A. and Ifelebuegu A.O. (2020). Kinetics Isotherms and Thermodynamic Modeling of the Adsorption of Phosphates from Model Wastewater Using Recycled Brick Waste. Processes, **8**, 665. https://doi.org/10.3390/pr8060665

Elewa A.M., Amer A.A., Attallah M.F., Gad H.A., Al-Ahmed Z.A.M., Ahmed I.A. (2021). Chemically Activated Carbon Based on Biomass for Adsorption of Fe(III) and Mn(II) Ions from Aqueous Solution. Materials, **16**, 1251. https://doi.org/10.3390/ma16031251

Fakhar N., Khan S.A., Siddiqi W.A. and Khan T.A. (2021). Ziziphus jujube waste-derived biomass as cost-effective adsorbent for the sequestration of Cd^{2+} from aqueous solution: Isotherm and kinetics studies. Environmental Nanotechnology, *Monitoring & Management*, **16**, 100570. Doi: https://doi.org/10.1016/j.enmm.2021.100570

Fideles R.A., Teodoro F.S., Xavier A.L.P, Adarme O.F.H., Gil L.F. and Gurgel A.V.A (2019). Trimellitated sugarcane bagasse: A versatile adsorbent for removal of cationic dyes from aqueous solution. Part II: Batch and continuous adsorption in a bicomponent system, *Journal of Colloid and Interface Science*, **552** (15), 752–763. https://doi.org/10.1016/j.jcis.2019.05.089

Foday Jr.E.H., Bo B., Xu X. (2021). Removal of Toxic Heavy Metals from Contaminated Aqueous Solutions Using Seaweeds: A Review. Sustainability, **13**, 12311. https://doi.org/10.3390/su132112311

Hasani N., Selimi T., Mele A., Thaçi V., Halili J., Berisha A. and Sadiku M. (2022). Theoretical S.M., Equilibrium, Kinetics and Thermodynamic Investigations of Methylene Blue Adsorption onto Lignite Coal. *Molecules*, **27**, 1856. https://doi.org/10.3390/molecules27061856

Hong J., Xie J., Mirshahghassemi S., Lead J. (2020). Metal (Cu, Cr, Ni, Pb) removal from environmentally relevant waters using polyvinylpyrrolidone – coated magnetic nanoparticles. *RSC advances*, **10**, 3266–3276. Doi: https://doi.org/10.1039/C9RA10104G

Ibuot A., Dean A.P., McIntosh O.A. and Pittman J.K. (2017). Metal bioremediation by CrMTP4 over-expressing Chlamydomonas reinhardtii in comparison to natural wastewater-tolerant microalgae strains. *Algal Research*, **24**, 89–96. https://doi.org/10.1016/j.algal.2017.03.002

Ji L., Xie S., Feng J., Li Y. and Chen L. (2012). Heavy metal uptake capacities by the common freshwater green alga Cladophora fracta, *Journal of Applied Psychology*, **24**, 979–983. https://doi.org/10.1007/s10811-011-9721-0

Katiyar R., Patel A.K., Thanh-Binh N., Singhania R.R., Chiu-Wen C. and Cheng-Di D. (2021). Adsorption of copper (II) in aqueous solution using biochars derived from Ascophyllum nodosum seaweed. *Bioresource Technology*, **328**, 124829. https://doi.org/10.1016/j.biortech.2021.124829

Khan N., Wahid F., Sultana Q., Saqib N.U. and Rahim M. (2020). Surface oxidized and un-oxidized activated carbon derived from Ziziphus jujube Stem, and its application in removal of Cd (II) and Pb (II) from aqueous media. *SN Applied Sciences*, **2**, 753. Doi: https://doi.org/10.1007/s42452-020-2578-6

Khan T.A., Noumana M.D., Dua D., Khan S.A. and Alharthi S.S. (2022). Adsorptive scavenging of cationic dyes from aquatic phase by H_3PO_4 activated Indian jujube (Ziziphus mauritiana) seeds based activated carbon: Isotherm, kinetics, and thermodynamic study, *Journal of Saudi Chemical Society*, **26** (2), 101417. https://doi.org/10.1016/j.jscs.2021.101417

Kharel H.L., Shrestha I., Tan M., Nikookar M., Saraei N., Selvaratnam T. (2023). Cyanidiales-Based Bioremediation of Heavy Metals. *BioTech*, **12**, 29. https://doi.org/10.3390/biotech12020029

Labied R., Benturki O., Hamitouche A.Y.E and Donnot A. (2018). Adsorption of hexavalent chromium by activated carbon obtained from a waste lignocellulosic material (Ziziphus jujuba cores): Kinetic, equilibrium, and thermodynamic study. *Adsorption Science and Technology*, **36** (3-4), 1066–1099. Doi:10.1177/0263617417750739

León G., Gómez E., Miguel B., Hidalgo A.M., Gómez M., Murcia M.D., Guzmán M.A. (2022). Feasibility of Adsorption Kinetic Models to Study Carrier-Mediated Transport of Heavy Metal Ions in Emulsion Liquid Membranes. *Membranes*, **12**, 66. https://doi.org/10.3390/membranes12010066

Lin Z., Li J., Luan Y., Dai W. (2020). Application of algae for heavy metal adsorption: A 20-year meta-analysis. *Ecotoxicology and Environmental Safety*, **190**, 110089. https://doi.org/10.1016/j.ecoenv.2019.110089

Ma J., Hou L., Li P., Zhang S. and Zheng X. (2022). Modified fruit pericarp as an effective biosorbent for removing azo dye from aqueous solution: study of adsorption properties and mechanisms, *Environmental Engineering Research*, **27** (2), 200634. https://doi.org/10.4491/eer.2020.634

Marah W., Khalid., Sami D. and Salman (2019). Adsorption of Heavy Metals from Aqueous Solution onto Sawdust Activated Carbon. *Al-Khwarizmi Engineering Journal*, **15** (3), 60–69. https://doi.org/10.22153/kej.2019.04.001

Mustapha S., Shuaib D.T., Ndamitso M.M. et al. (2019). Adsorption isotherm, kinetic and thermodynamic studies for the removal of Pb(II), Cd(II), Zn(II) and Cu(II) ions from aqueous solutions using Albizia lebbeck pods. *Applied Water Science,* **9**, 142. https://doi.org/10.1007/s13201-019-1021-x

Olawale S.A., Bonilla-Petriciolet A., Mendoza-Castillo D.I., Okafor C.C., Sellaoui L. and Badawi M. (2022). Thermodynamics and Mechanism of the Adsorption of Heavy Metal Ions on Keratin Biomasses for Wastewater Detoxification, *Adsorption Science and Technology*, ID 7384924. https://doi.org/10.1155/2022/7384924

Omer M., Khan B., Khan I., Alamzeb M., Zada F.M., Ullah I., Shah R., Alqarni M., Simal-Gandara J. (2022). Kinetic and Thermodynamic Studies for the Adsorption of Metanil Yellow Using Carbonized Pistachio Shell-Magnetic Nanoparticles. *Water*, **14**, 4139. https://doi.org/10.3390/w14244139

Pereira S.K., Kini S., Prabhu B. *et al*. (2023). A simplified modeling procedure for adsorption at varying pH conditions using the

modified Langmuir–Freundlich isotherm. Appl Water Sci 13, 29. https://doi.org/10.1007/s13201-022-01800-6

Shafiq M., Alazba A.A., Amin M.T. (2021). Kinetic and Isotherm Studies of Ni^{2+} and Pb^{2+} Adsorption from Synthetic Wastewater Using Eucalyptus camdulensis—Derived Biochar. *Sustainability*, **13**, 3785. https://doi.org/10.3390/su13073785

Su L., Zhang H., Oh K., Liu N., Luo Y., Cheng H., Zhang G. and He X. (2021). Activated biochar derived from spent Auricularia auricula substrate for the efficient adsorption of cationic azo dyes from single and binary adsorptive systems, *Water Science & Technology*, **84**, (1), 101–21. https://doi.org/10.2166/wst.2021.222

Venkatraman Y. and Priya A.K. (2021). Removal of heavy metal ion concentrations from the wastewater using tobacco leaves coated with iron oxide nanoparticles, *International Journal of Environmental Science and Technology*, **19**, 2721–2736. https://doi.org/10.1007/s13762-021-03202-8

Wang J. and Guo X. (2023). Adsorption kinetics and isotherm models of heavy metals by various adsorbents: An overview. *Critical Reviews in Environmental Science and Technology*, https://doi.org/10.1080/10643389.2023.2221157

Yahya M.D., Aliyu A.S., Obayomi K.S., Olugbenga A.G. and Abdullahi U.B. (2020). Column adsorption study for the removal of chromium and manganese from electroplating wastewater using cashew nutshell adsorbent. *Chemical engineering* **7,** 1748470. Doi: https://doi.org/10.1080/23311916.2020.1748470

Yogeshwaran V. and Priya A.K. (2021). Experimental studies on the removal of heavy metal ion concentration using sugarcane bagasse in batch adsorption process, *Desalination and Water Treatment*, **224**, 256–272. https://doi.org/10.5004/dwt.2021.27160

Yu H., Liu Y., Shu X. *et al*. (2020). Equilibrium, kinetic and thermodynamic studies on the adsorption of atrazine in soils of the water fluctuation zone in the Three-Gorges Reservoir. *Environmental Sciences Europe* **32**, 27 https://doi.org/10.1186/s12302-020-00303-y